Coupled Systems Mechanics, *Vol. 12, No. 5 (2023) 461-479*
https://doi.org/10.12989/csm.2023.12.5.461

On soil-structure interaction models to simulate free vibrations and behavior under seismic loads of a RC building supported by a particular shallow foundation

Soelarso Soelarso[1,3], Jean-Louis Batoz*[2], Eduard Antaluca[1] and Fabien Lamarque[1]

[1]*Laboratoire Avenues, Université de Technologie de Compiègne, Alliance Sorbonne Université, CS 60319, 60203 Compiègne, France*
[2]*Laboratoire Roberval, Université de Technologie de Compiègne, Alliance Sorbonne Université, CS 60319, 60203 Compiègne, France*
[3]*Civil Engineering, Sultan Ageng Tirtayasa University, Jl. Jenderal Sudirman Km 3, Cilegon 42435, Indonesia*

(Received April 1, 2023, Revised June 12, 2023, Accepted July 21, 2023)

Abstract. The paper deals with the finite element modelling of the free vibration and structural behavior of a particular four-floor reinforced concrete structure subjected to static equivalent seismic loads and supported by a shallow foundation system called SNSF (Spider Net System Footing). The two FE models are a simple 2D Matlab model and a detailed 3D model based on solid elastic elements using Altairworks (Hypermesh and Optistruct). Both models can simulate the soil structure interaction. We concentrate on the behavior of a representative cell involving two columns on five levels. The influence of the boundary conditions on the external vertical planes of the domain are duly studied. The Matlab model appears relevant for a primary estimation of frequencies and stiffness of the whole structure under vertical and lateral loads.

Keywords: altairworks; finite element modelling; free vibration; hypermesh software; Matlab software; Optistruct software; seismic loads; shallow foundation system SNSF

1. Introduction

In Soelarso *et al.* (2021), we described a particular shallow foundation system called SNSF (Spider Net System Footing) frequently used in building construction in Indonesia and well suited for foundation on soft soils (https://www.katama.co.id/). The SNSF system is claimed to be economical and earthquake resistant since it acts in a monolithic way with the upper structure with respect to soil structure interaction. Limited damages (like differential settlements) have been observed in existing buildings subjected to seismic actions. However, limited reports or papers have been published on the subject and detailed analyses using advanced computational mechanics approaches have not been performed so far to quantify the soil-structure interaction in the presence of SNSF shallow foundations.

*Corresponding author, Professor, E-mail: jean-louis.batoz@utc.fr

http://www.techno-press.org/?journal=csm&subpage=8 ISSN: 2234-2184 (Print), 2234-2192 (Online)

In an earlier contribution (Soelarso *et al.* 2019) we did consider a unit SNSF cell subjected to a central load. That cell was investigated by Darjanto (2015), Darjanto *et al.* (2015) both experimentally and numerically. We modelled the cell using 3D solids elements and also shell elements. We took into account the supported soil with different dimensions. The results we obtained taking into account the soil structure interaction were in good agreement with the available experimental results for the range of elastic behavior of the soil. The paper Soelarso *et al.* (2022) was the focused on the Finite Element (FE) modeling of a rectangular slab lying on multilayer elastic soil (see Cuira and Simon 2008) in order to study the influence of the element types, the influence of contact conditions (sliding or sticking) at the interface of soil and structure. Good agreement with the results reported in Cuira and Simon (2008) for that particular example of soil structure interaction was encouraging to model more complicated problems with the assumption of sticking contact between the soil and the upper structure. Hence in 2021 (Soelarso *et al.* 2021) we started to consider a real building supported by the SNSF shallow foundation. In that first contribution (details given in section 2) we focused on the static analysis of a single cell of the building involving one column and we made à first evaluation of the lowest frequencies of the upper structure.

In the present paper we consider the same building but we define another cell involving two columns to propose a first modelling of that cell understee seismic equivalent lateral loads following the general recommendation of EC8 (Eurocode 8 2004) or ACI (ACI 2015), see also Jalil and Jalil (2019), Davidovici (2015). That approach is based on the use of an elastic response spectrum and needs an estimation of the lowest frequency of the upper structure (including possibly the influence of the foundation system and supporting soil). That aspect justifies the content of section 3 on free vibrations. Section 4 is devoted to the modelling of a particular cell involving two columns, the estimation of equivalent seismic loads and the estimation of 3D displacements and stresses. All results are based on the assumption of 3D elasticity for the structure, for the SNSF foundation and supporting soil.

The 3D FEM models are obtained using advanced FE and CAD software from the Altair Hyperworks Platform (like Hypermesh and Optistruct) (https://www.altairhyperworks.com) and from Autodesk (Revit, Robot Structural Analysis) (https://www.autodesk.com). The soil structure interactions assume full contact on the interfaces of the RC structure and supporting soil. We

Fig. 1 3D view of the UNTIRTA Campus, including the economy building

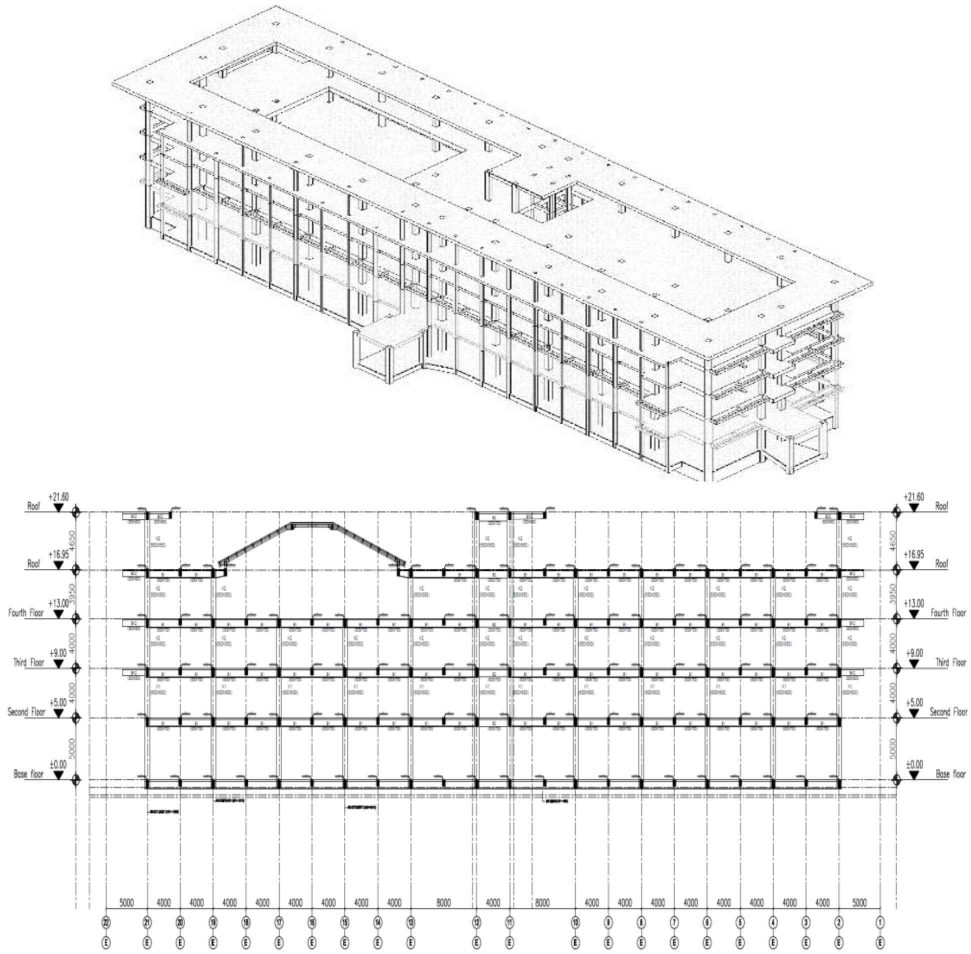

Fig. 2 Economy Building (3D view and cross section)

assume linear elasticity and classical 3D finite elements as described in FEM textbooks, such as Batoz and Dhatt (1990), Bathe (2016), Ibrahimbegovic (2009).

We also propose Matlab models based on the modeling of the columns using "exact" Timoshenko beams, (Batoz and Dhatt 1990, Ibrahimbegovic 2009), with only one degree of freedom (the horizontal displacement at each floor level) and using simple linear shear beam elements to represent the supporting soft and hard soils.

2. Description of a single cell

As in Soelarso *et al.* (2021), we consider the economy building on the UNTIRTA Campus project in the Banten province on Java Island (Indonesia). We briefly recall the main geometrical characteristics for a better understanding of the following sections. Figs. 1 and 2 present the Reinforced Concrete (RC) building erected in 2020. That four-floor (plus the ground floor) building has a length of 84 m and 23 m width. The upper floor slabs are supported by 48 inside

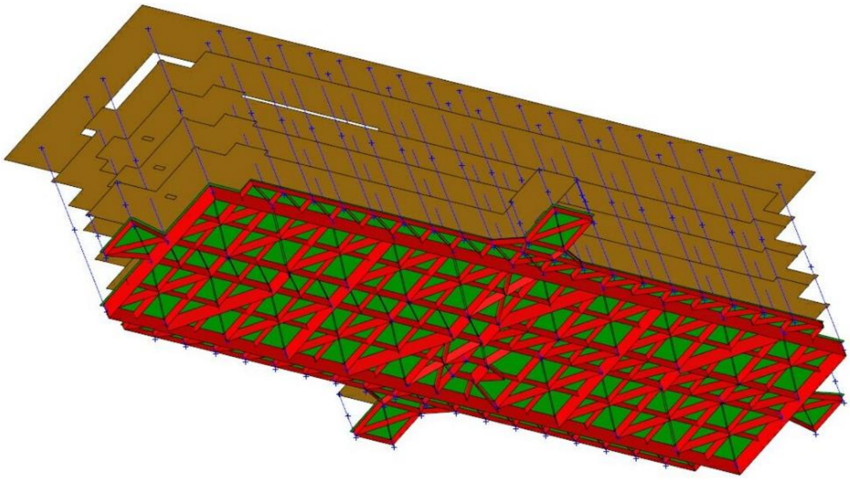

Fig. 3 3D view of the building showing the upper structure and the SNSF foundation system (in red)

Table 1 Material properties of soil and concrete

Material	Elasticity Modulus (E) (MPa)	Density (T/m^3)	Shear Modulus (G) (MPa)	Poisson
Concrete	21409 (*fc*=20 MPa)	2.4	8234	0.2
Soft soil (2 m)	11	1.74	4.6	0.3
Hard soil (9 m)	27	1.75	28.85	0.3

columns having a square cross-section of 0.6 m by 0.6 m. Fig. 3 shows the SNSF foundation (in red) and the upper structure (in brown). Fig. 4 shows a top view of the SNSF foundation under the horizontal slab at the ground floor level. Fig. 4 also presents one SNSF cell involving two columns of 17 m height with a square cross-section (0.6 m×0.6 m) and four floors (first floor at 5 m from ground level, upper levels 4 m height each). The chosen cell with dimensions 8 m (in X-direction) and 11 m in (in Y-direction) is extracted from the whole structural system. We assume that the chosen cell is a valuable representation of the structural behavior of the whole building and we will precise later the boundary conditions between that cell and the neighboring ones. The upper floors and the roof involve orthogonal girders (beams of cross sections of 0.3 m×0.7 m or 0.3 m×0.5 m). They support the floor slabs of 0.13 m thickness or the roof slab of 0.1 m thickness. Fig. 4 clearly shows (in the lower right part) that one SNSF cell is made of several RC vertical ribs of 0.11 m thickness with different heights (between 0.80 m for the inside ribs up to 2 m for the limit ribs), (Mohy 2017). The hard soil is located 2 m below the ground floor level. The 2 m excavated soil is used to subsequently fill the 12 sub-cells located between the ribs and then compacted before carrying out the RC slab to close the cells. In Soelarso *et al.* (2021), we did consider a smaller cell (7mx8m) involving only one column.

3. Free vibrations of an SNSF cell, including two columns under soft soil.

In the previous paper by Soelarso *et al.* (2021), we studied the influence of different FEM models (2D beam or 3D FEM), different types of foundations (raft, SNSF, piles) using different

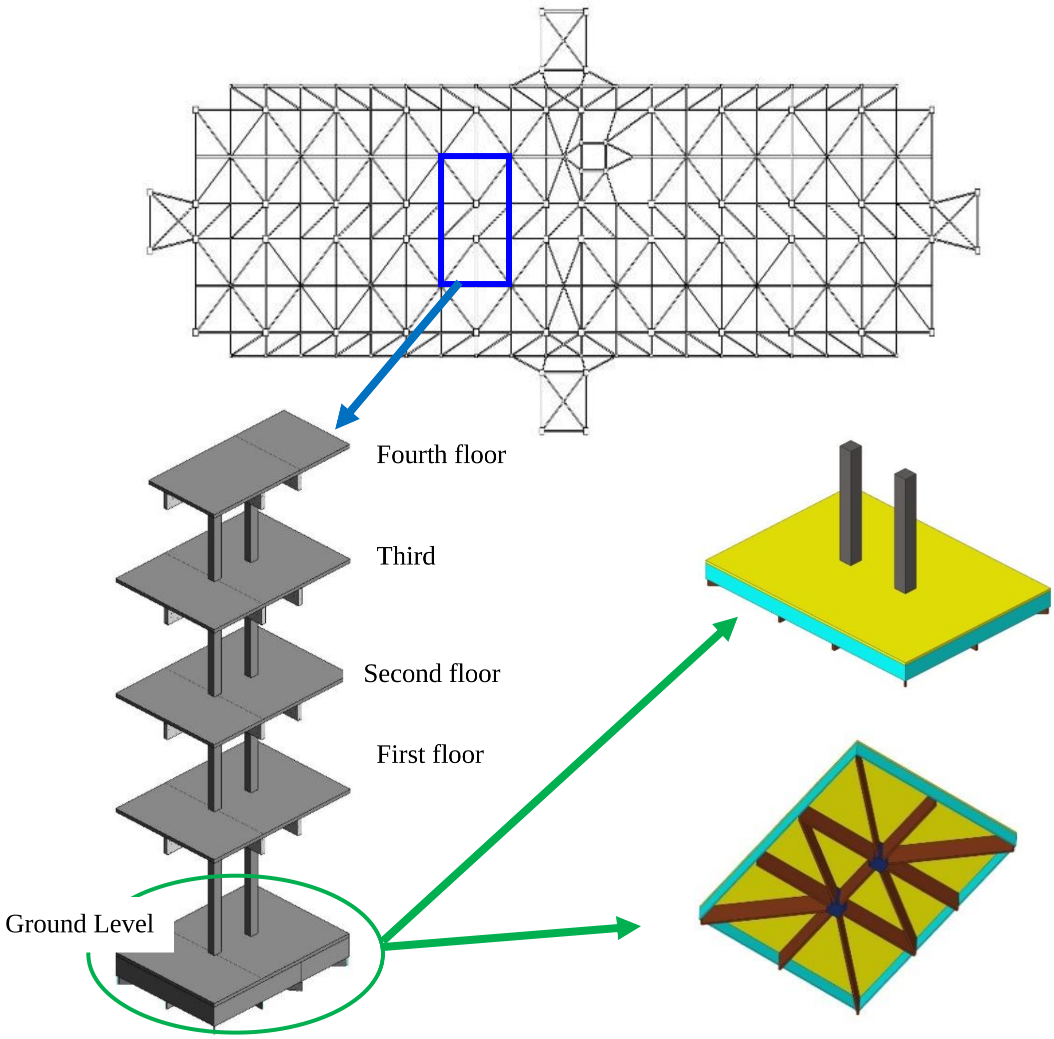

Fig. 4 Top view at the floor level and location of one SNSF cell with two columns

software (Matlab, Autodesk Robot, Altair Works) to conclude that a fair estimation of the lowest frequencies can be estimated using a 2D beam Matlab model considering a simple geometrical cell representative of the structure. In this section, we present more details on the Matlab model and we consider different dimensions of the cell, including the two columns, as represented in Fig. 4.

We assume linear homogeneous elastic properties for the concrete and the two types of soil (Table 1). Full continuity of displacements (sticking contact) is assumed between the soil and the reinforced concrete surfaces, after a study of the influence of contact conditions on the soil-structure surface.

Fig. 5 represents a model of one cell with the upper structure, the two columns on the SNSF support with details of the dead (permanent) loads and live loads acting on each floor level. The masses are deduced from the loads acting on each floor with their corresponding two columns (without weighting factors). Fig. 6 represents a "brochette" model of the upper structure, in a 2D

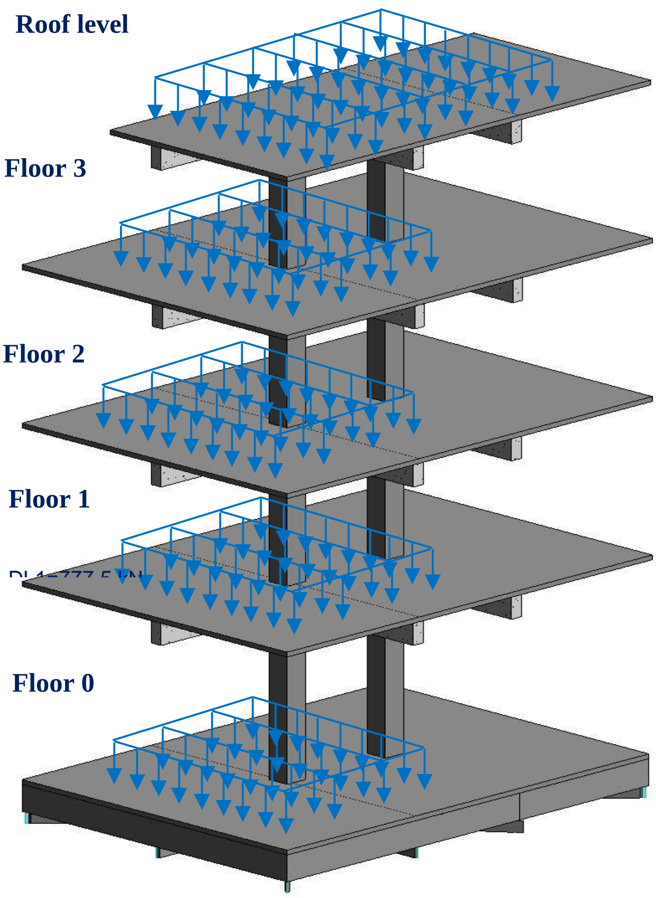

Fig. 5 Dead load and live loads on a cell (structure+SNSF) involving two columns and five levels

XZ-plane, with four elements (for the two columns). We assume that the slabs are infinitely rigid and moves horizontally (the model involves only the horizontal displacement at the nodes). The stiffness matrix is the "exact" 2D stiffness of the Timoshenko beam element, including transverse shear effects (see Batoz and Dhatt 1990). The element stiffness K_i is then given by

$$K_i=\frac{12\,H_f}{L^3(1+\emptyset)} \quad \text{with } H_f=EI; \quad \emptyset=\frac{12.H_f}{L^2 H_c} \;;\; H_c=k.G.A \;;\; k=5/6 \qquad (1)$$
$$L=4 \text{ m for } K_2;\, K_3;\, K_4. \text{ and } L=5 \text{ m for } K_1$$

($I=\frac{2\,a^4}{12}$ and A=2 a^4 represent the moment of inertia and cross-sectional area respectively, for two columns that bend in the YZ-plane. Here, 'a' denotes the side length of the column's cross-section).

In a 2D model, the soil can be simply represented by two nodes shear beam elements with element stiffness K_{si}

$$K_{si}=G_i(i)\ \text{Area}(i)/l(i) \qquad (2)$$

i corresponds to a specific layer of soil with $G(i)$ the shear modulus (Table 1), Area(i) the

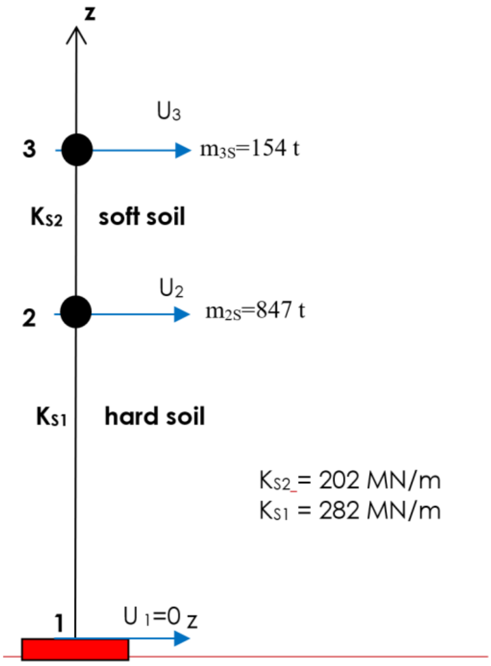

Fig. 6 Shear beam model of the soil layers

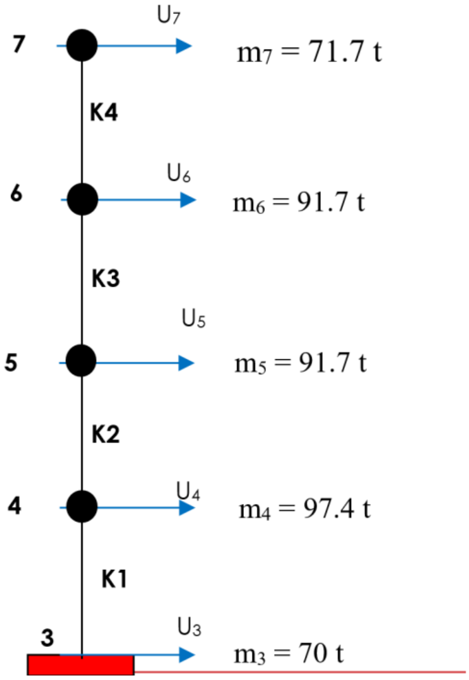

Fig. 7 2D Beam "brochette" model of the structure

surface area of the soil under the upper columns and *l(i)* the length of the soil element in the vertical direction. In this case, the dimensions of the cell are such that Area=8×11=88 m^2; l=2 m for the soft soil and l=9 m for the hard soil (more elements can be considered to represent the soil, but results will not change).

The total mass of a soil element is simply given by its volume V_e times the volumic mass $\boldsymbol{\rho_e}$. Hence the concentrated mass at each node i is given by

$$Msoil\ (i) = (V_e \cdot \rho_e)/2 \qquad (3)$$

With the above simple models (Figs. 6 and 7), the contribution of the soil to the free vibration of the construction system can be estimated. Table 2 reports our results: column 2 gives the first four frequencies for the upper structure alone using beam elements; almost the same results can be obtained using 3D finite elements, and the corresponding mode shapes are shown in Fig. 8; column 3 reports the results for the first two frequencies of the two layers of soil alone; column 4 reports the frequencies obtained considering a "brochette" model including the upper structure (Fig. 7) with four beam elements and the supporting soil with two shear soil elements (a total of only 6 dof !). The frequencies are lower than those of the structure alone. For the fundamental frequency, the ratio f_{1b+s}/f_b=1.26/1.44=0.875 value is in good agreement with reference values given in (Jalil and Jalil 2019, see Figs. 2.4.4.2 page 35). Our Matlab results are independent of the number of elements but depend on the assumed Area A (for example, $f1$=1.26 Hz for A=88 m^2 and 1.14 Hz for A=44 m^2).

The results shown in Table 2 can be compared with those obtained considering a refined 3D finite element model using Revit (https://www.autodesk.com), Hypermesh and Optistruct (https://www.altair.com/hyperworks), as shown in Fig. 9. The present FEM model (see also Fig. 4)

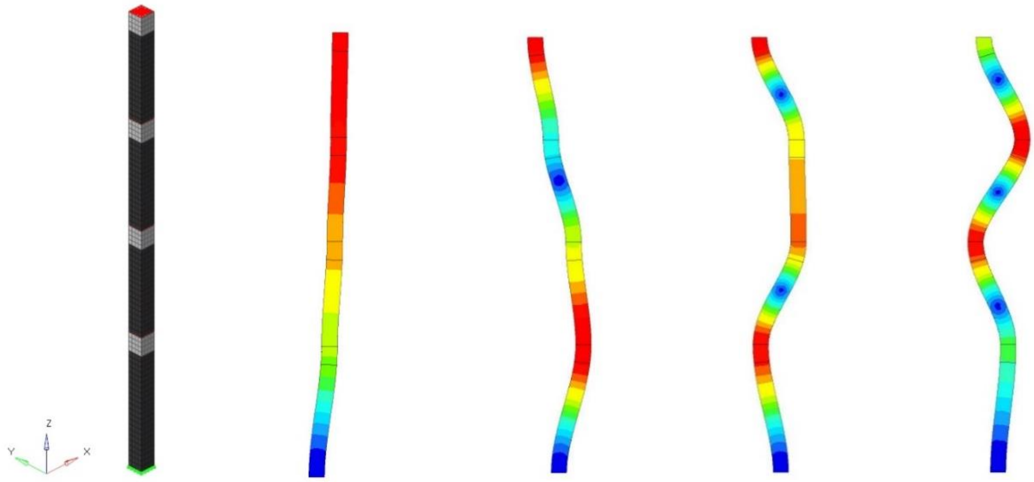

Fig. 8 3D elasticity models and mode shapes of the four-floor structure

Table 2 Frequencies using the Matlab models

f in Hz	Upper structure alone (4 elements)	Soil alone One element for each layer of soil Area=88 m^2	Upper structure+One element for each layer of soil Area=88 m^2
f_1	f_{1b}=1.44	2.62 (T_1=0.38 s)	f_{1b+s}=1.26
f_2	4.40	6.41 (T_2=0.156 s)	2.69
f_3	7.09		4.36
f_4	8.88		5.92

involves 3408 H8 elements for the floor junctions, 33575 H8 for the columns, 12728 for the SNSF structure, 6196 for the slab, 55764 for the hard soil, 55764 for the soft soil and 32232 elements for the compacted soil inside the cells of the SNSF. The total number of elements is 213608 for a total of 223765 nodes (670000 dof).

The frequencies depend on the assumptions on the external vertical surfaces (Table 3). Hence, we consider four cases: sym/sym means symmetry conditions on the four external vertical planes of the cell (Fig. 9), free/free means no boundary conditions on the vertical planes, then we add results for symmetry conditions on the YZ external planes (11 m length) and free on XZ-plane (8 m length), we also include results for symmetry conditions on the XZ external planes (8 m length) and free on YZ-plane (11 m length). Symmetry conditions on the YZ opposite surfaces imply u=0 at any node of those surfaces, while symmetry conditions on the XZ opposite surfaces imply v=0 at any node of those surfaces.

Table 3 shows that including the soil and foundation leads to a reduction of the frequencies for all four assumptions of boundary conditions on the external vertical planes. For example, considering the Free/Free assumption (f=0.95 for the first frequency), the ratio f/f_{1b}=0.95/1.42=0.67. However, if we consider the Sym/sym assumption (f=1.35), the ratio f/f_{1b}=1.35/1.42=0.95. Comparing Tables 2 and 3, we can also observe that the simple Matlab model

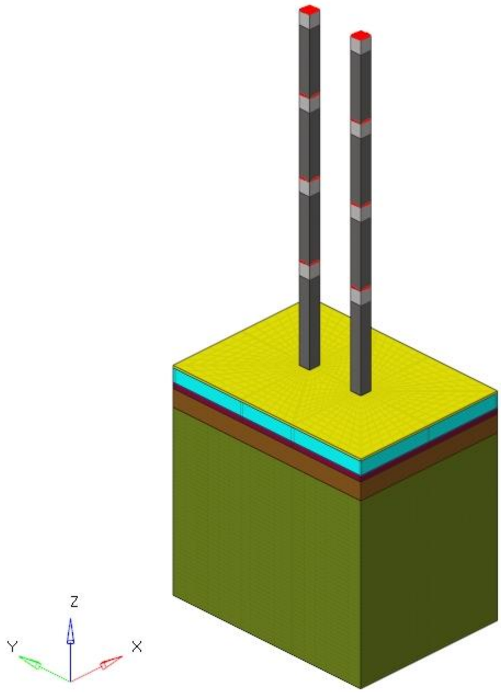

Fig. 9 3D FE Elasticity model with SNSF foundation, soft and hard soil

Table 3 Frequencies of one SNSF cell with two columns

Mode	Frequency (Hz)				
	Upper structure alone	SNSF cell			
		Sym/sym	Free/free	YZ-plane sym/ XZ-plane free	XZ-plane sym/ YZ-plane free
1	f_{1b}=1.42	1.35	0.95	1.08	0.99
2	1.42	1.35	1.07	1.35	1.35
3		1.36	1.33	1.35	1.36
4		1.37	1.36	1.37	1.37
5		3.84	2.23	2.40	2.24
6	4.35	4.35	2.38	3.55	3.56
7	4.35	4.36	2.60	4.31	4.27
8		4.37	3.42	4.36	4.35

(Table 2) leads to a reduction of the frequency with the same order of magnitude as in Table 3 (f/f_{1b}=1.26/1.44=0.875).

4. Static analysis of one SNSF cell under equivalent lateral and vertical seismic loads

Instead of using a step-by-step dynamic analysis driven by a given accelerogram, in this section we will consider an equivalent static approach according to the EC8 or ACI design codes (or the

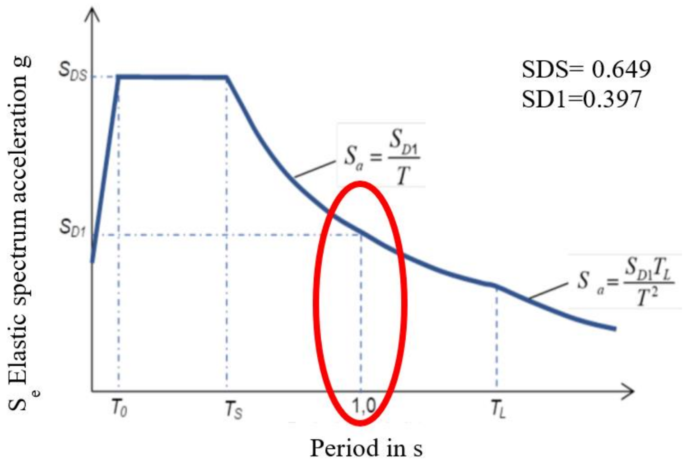

Fig. 10 Elastic response spectrum

SNI (2019) in the context of Indonesia), Charney (2015), Eurocode 8 (2015), Davidovici *et al.* (2015), Ponginan (2018), Jalil and Jalil (2019). We apply the procedure considering the economy building on the campus of UNTIRTA. As in the previous section, we consider and study the influence of the SNSF foundations and compare the results with those of the upper structure alone. The first step is the definition of the elastic response spectrum to estimate the amplification of acceleration due to seismic motion. Then we define the equivalent lateral static loads on the structure and study the structure together with the SNSF foundation, also taking into account the action of the vertical loads due to dead and live loads.

4.1 Elastic response spectrum

The influencing parameters for the elastic response spectrum are mainly the seismicity zone, and the soil classification. For our study, we consider "moderate to high seismicity" and a "medium-stiff" soil, corresponding to a bearing capacity in the range c_u=0.07-0.25 MPa. According to the dynamic design codes, the response spectrum is presented in Fig. 10.

We recall that for the free vibration analysis, the first frequency was estimated as follows:

- 0.97 Hz for the upper structure alone (using Autodesk Robot Structural Analysis)
- 1.44 Hz for the upper structure alone (using a 2D Matlab model or a 3D FEM for one column)
- between 1.35 and 0.95 Hz (average 1.15 Hz) using a 3D FEM model of one cell, including the SNSF and the supporting soil.

Hence, we propose to use 1 Hz for the fundamental frequency using the elastic response spectrum. As a consequence, the amplification of acceleration due to the seismic motion is given by

$$S_{D1}=0.397\text{ g}=3.89\text{ m/s}^2 \tag{4}$$

4.2 Static equivalent lateral loads

The dead and live loads are shown in Fig. 5. The total value of the permanent loads from level

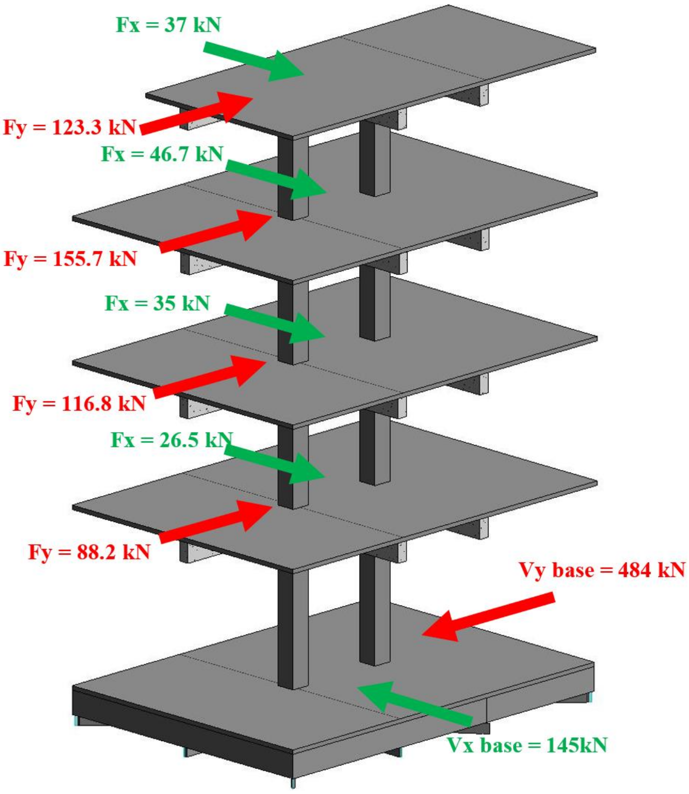

Fig. 11 Static equivalent forces on each column of the SNSF cell

1 to level 4 are equal to 2673 kN, and the total live load from level 1 to level 4 is 824 kN.

The total mass of the cell for the seismic action, according to the EC8 proposal, is

$$M=(2673+\mathbf{0.24}\times 824)/9.81=293 \text{ t}. \tag{5}$$

The static equivalent lateral loads depend on the type of construction, the seismic importance factor, and the building priority factors, such as the risk category of the building. In the present academic study, we will not give details of the computation of the so-called Seismic response coefficient (C_s) used to define the amplitude of the Seismic shear base force V in terms of the effective seismic weight W (or mass M=W/g) of the cell structure above the ground level

$$V=C_s\times W=C_s \text{ M g} \tag{6}$$

As suggested in (Jalil and Jalil 2019), we consider rather arbitrarily, C_s=SD1×0.85=0.337, so that the total shear force is taken as V=968 kN (for a cell with two columns). Hence, for one column

$$V=484 \text{ kN} \tag{7}$$

The lateral seismic forces distribution is assumed in agreement with the shape of the fundamental mode of vibration of the upper structure. Hence, the horizontal load F_{yi} at floor i, in the y direction, is given by

$$F_{yi\,.}=V\;\; v_i\;.\;m_i/(\sum v_j\;.m_j) \tag{8}$$

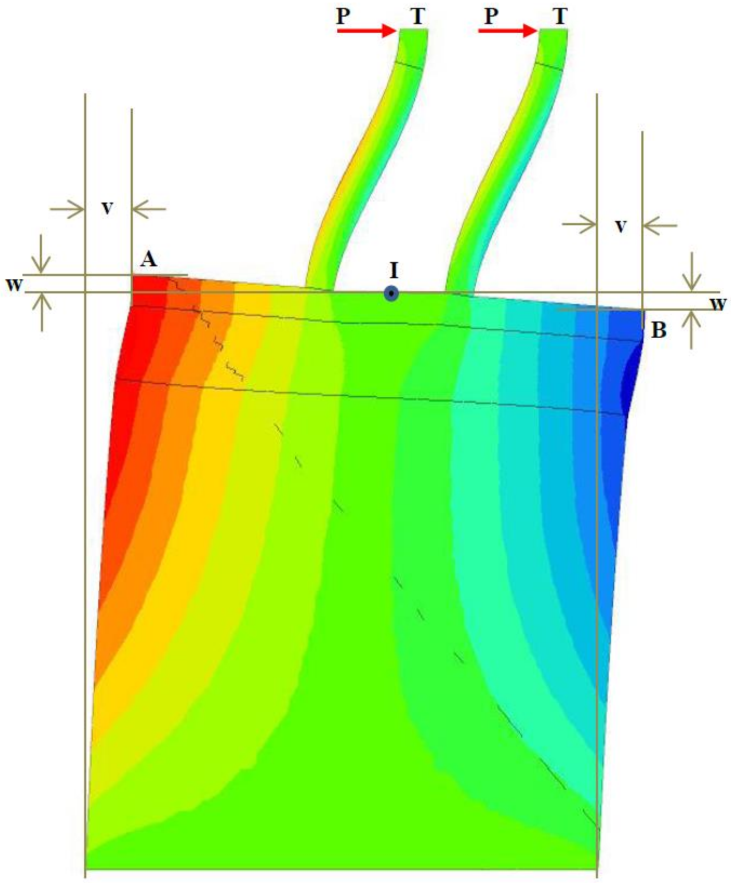

Fig. 12 Displacements v and w for a central vertical plane considering free/free boundary conditions

v_i and v_j are the modal displacements in Y-direction at floor i and j; m_i and m_j are the mass at levels i and j, in agreement with Eqs. (7) and (8). We consider m_4=42.19 t; m_5 =37.25 t; m_6=37.25 t; m_7=29.5 t.

The relative values of modal displacements for mode 1 are: v_4 =0.2; v_5 =0.3; v_6 =0.4; v_7 =0.4. The values of the horizontal forces in the Y-direction, to be applied at the four floors are then

$$F_{y4}=88.2\text{ kN};\ F_{y5}=116.8\text{ kN};\ F_{y6}=155.7\text{ kN};\ F_{y7}=123.3\text{ kN}; \tag{9}$$

According to the design codes, it is also necessary to simultaneously consider the action of lateral forces in the X-direction with values equal to 30% of the values in the Y-direction. The two types of forces are shown in Fig. 11 (green for X-direction, red color for Y-direction).

4.3 Static equivalent lateral analysis of one SNSF cell under lateral and vertical seismic loads

We consider a FE model similar to the previous one (Fig. 9). However when we assume that one cell is representative of the whole behavior of the structure, we cannot use the symmetry or the free conditions on the four vertical limit planes of the cell when the columns are in bending. In

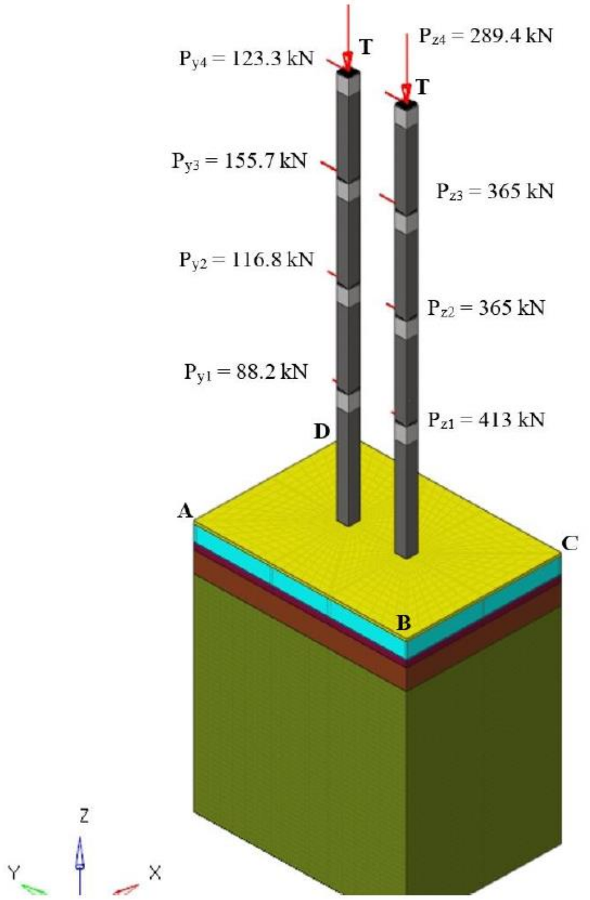

Fig. 13 Model with static equivalent lateral loads in Y and Z direction

Fig. 12, we present a 2D central YZ-plane of a cell subjected to lateral loads in the Y-direction, when we assume free/free conditions. It is clear that such a deformation is not compatible with that of the neighboring cells in the Y-direction. We have to constraint the limits of the cell in order that $w_A=w_B$ and $v_A=v_B$ for any Z value on the limit vertical planes. This type of constraints can be taken into account using Hyperworks under the name MPC (Multi Point Constraints).

Hence, we propose a 3D FEM model under the sym/MPC conditions considering also the slab-column intersections as rigid bodies. The loads are the concentrated lateral forces in the Y-direction (red color, Fig. 11), to be applied on each column/floor intersection of the two columns, and also the vertical forces due to the permanent loads in the dynamic context: the concentrated vertical forces in the -Z-direction at the column's nodes, and the self-weight of the SNSF, compacted soil, soft and hard soil. The concentrated vertical forces are for each column; see Fig. 13 (total 1432 kN)

$$F_{z1}=-413 \text{ kN};\quad F_{z2}=-365 \text{ kN};\quad F_{z3}=-365 \text{ kN};\quad F_{z4}=-289.4 \text{ kN}. \tag{10}$$

Values of displacements obtained at top T are: v=-28. mm and w=-11.01 mm, and values at points A, B, C and D are given in Table 4. These values are located at the columns bases meaning

Table 4 Displacements at points *A*, *B*, *C*, *D* for single and combined loads in Y and Z-directions

Points	Displacements under horizontal and vertical loads (mm)		Displacements under horizontal load (mm)		Displacements under vertical loads (mm)	
	w	*v*	*w*	*v*	*w*	*v*
A	-2.65	-3.00	0.01	-2.86	-2.657	-0.14
B	-2.65	-2.59	0.01	-2.86	-2.657	0.27
C	-2.67	-2,72	-0.01	-2.86	-2.657	0.14
D	-2.67	-3.13	-0.01	-2.86	-2.657	-0.27

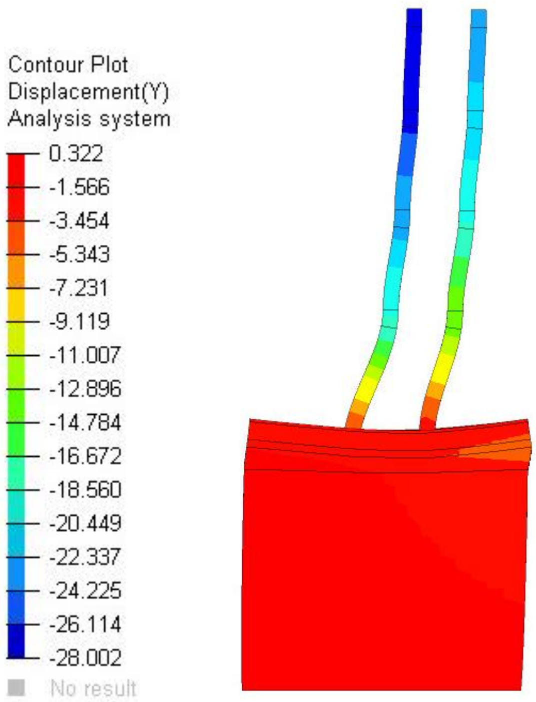

Fig. 14 Deformed shape in the YZ-plane

that the relative displacements from level 0 to top *T* are "reduced" to *w*=-11.01+2.65=-8.36 mm and to *v*=-28+2.86=-25.14 mm. Table 4 includes the results for horizontal loads and vertical loads separately. Fig. 14 shows the deformed model in the Y-direction. We can see that the MPC conditions are satisfied since $w_A=w_B=w_C=w_D$ and $v_A=v_B=v_C=v_D$ under lateral loads conditions.

We also use the six elements Matlab model of Figs. 6 and 7, considering the equivalent seismic loads of Fig. 13. For the gravity vertical loads model, we replace *G* with *E* for the two soil elements, and the structural elements are simple truss elements. Hence, the dofs are the vertical w displacements. The settlement at the basis is estimated to 13.5 mm, and the shortening of the column is around 2 mm. Under lateral loads in the Y-direction, the structural elements are the same as for the vibration (Timoshenko elements), and the horizontal loads are given in Fig. 13. The shear beam soil elements are free of charge. The Matlab results are larger than the 3D FEM ones i.e., 42 mm versus 28 mm. This is mainly attributed to the fact that the Matlab model is much less constrained than the 3D sym/MPC model.

Table 5 Displacements under seismic loads using the Matlab models

	Static vertical loads		Static lateral loads	
	Upper structure alone (4 elements)	Upper structure+ one element for each layer of soil; Area=88 m^2	Upper structure alone (4 elements)	Upper structure+ one element for each layer of soil; Area=88 m^2
Top	w=1.94 mm	w=15.43 mm	v=42 mm	v=50.23 mm
Basis	0	v=13.49 mm	0	v=8.21 mm

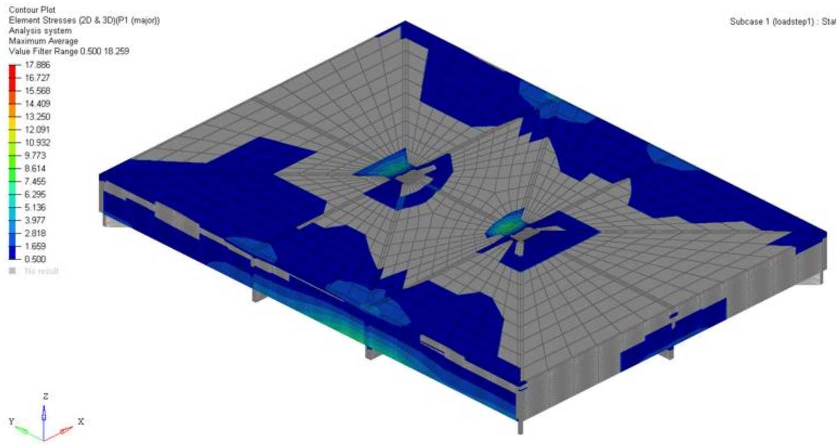

(a) P1 principal stresses (maximum in tension), top of slab, actions of forces in Y and Z-directions

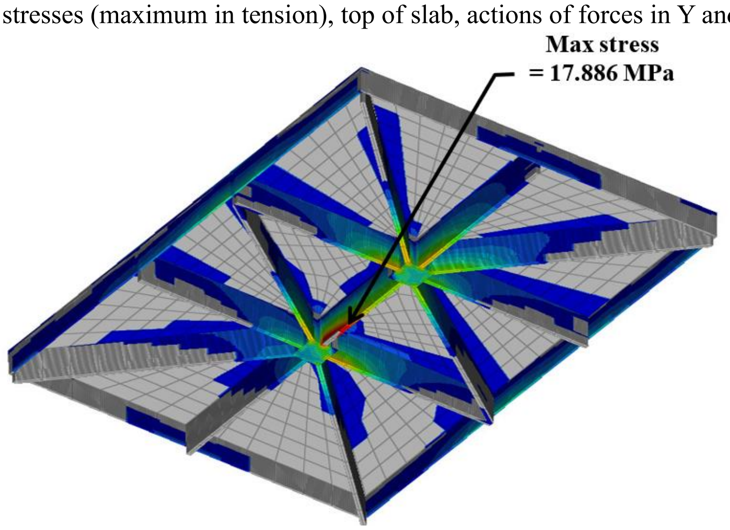

(b) P1 principal stresses (maximum in tension), below the slab, actions of forces in Y and Z-directions

Fig. 15 P1 principal stresses under combined actions of forces in Y and Z-directions

The principal stresses in the SNSF under the loads in Y and Z-directions (Fig. 13) are shown in Figs. 15 and 16. The maximum tension stress of 17.9 MPa is located in a lower part of a central rib, and the maximum stress in compression of -13.6 MPa is found on the top surface of the slab. Steel reinforcements will be necessary in the vertical RC ribs near the bases of the central columns (Davidovici *et al.* 2015).

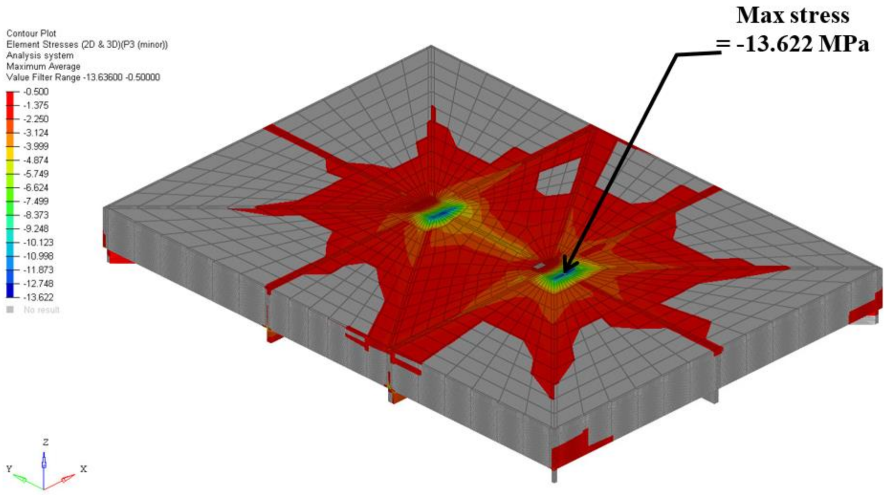

(a) P3 principal stresses (maximum in compression), top of slab, forces in Y and Z-directions

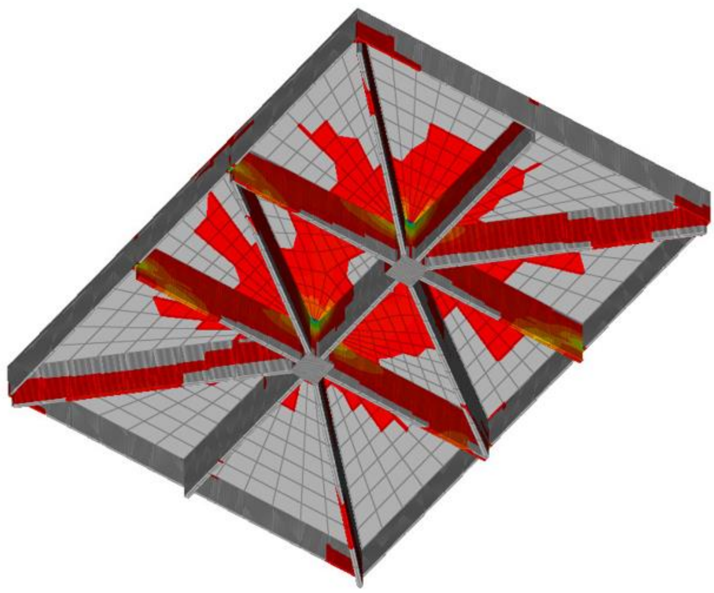

(b) P3 principal stresses (maximum in compression), under the slab, forces in Y and Z-directions

Fig. 16 P3 principal stresses under combined actions of forces in Y and Z-directions

The distribution of reaction stress σ_{zz} along the central YZ-plane is shown in Figs. 17 and 18. The average value is in agreement with a simple calculation of the compression stress due to the self-weight of the slab (40.8 t), of the compacted soil of one meter inside the SNSF (153 t) and the total vertical loads on the cell (293 t). The maximum stress of 0.08 MPa is well below the allowable bearing capacity (0.19 MPa).

The action of the lateral forces in the X-direction (Fig. 11) has not been included and superposed to the previous actions (*Fy* and *Fz*) because the constraints on the external surfaces are not the same. For bending actions in the XZ-plane, we need a model with symmetry on the XZ-

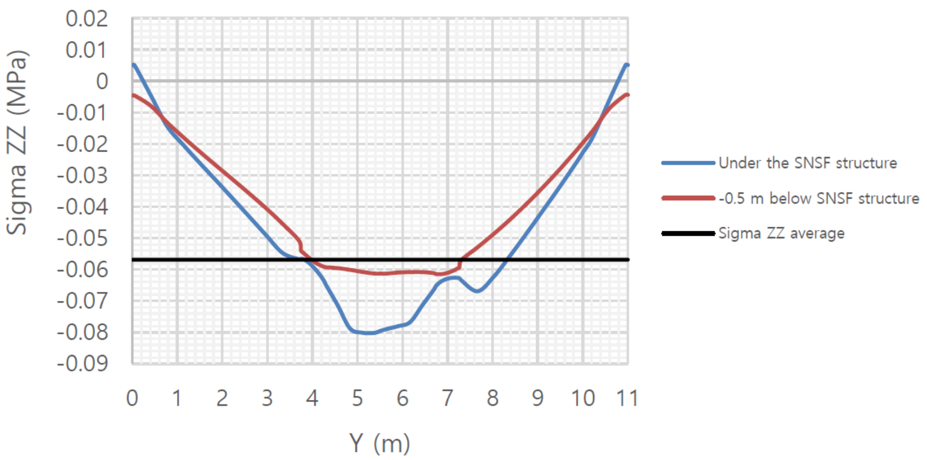

Fig. 17 Stress reactions σ_{zz} at bottom of the SNSF in Y central directions, for combined actions of the lateral loads in Y direction and Z-directions (*Fz*+self weight of foundation+soil)

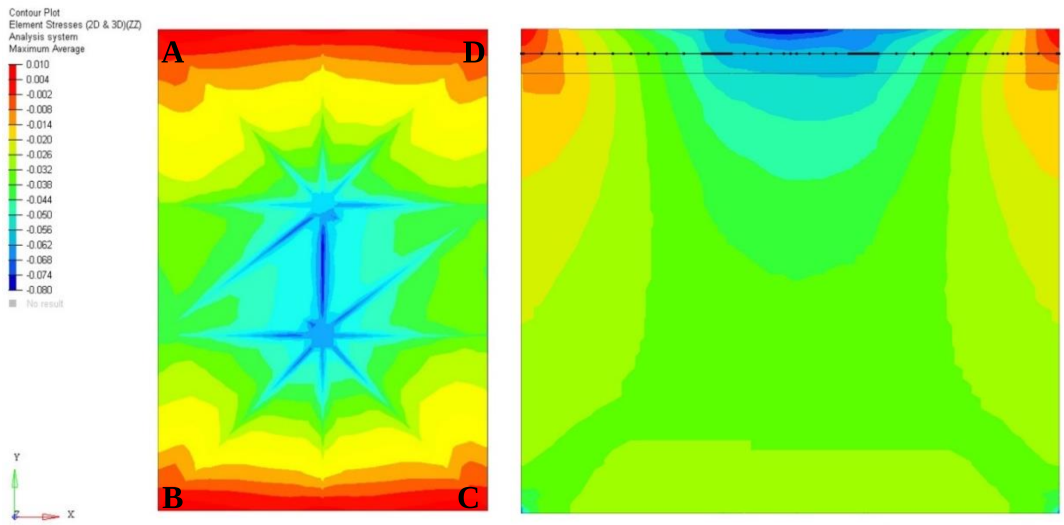

Fig. 18 Iso-values of σ_{zz} on the contact surface of SNSF and soil and in the soil depth

planes and MPC on each XY-plane in the Z-direction. We have performed such analysis, and the main results are as follows:

- u=0.85 mm for the foundation and u=7.75 mm on top T,
- the reactions stresses are positive and negative but the average is zero (but this is without the contribution of the vertical gravity loads !) ,
- the maximum stresses in the SNSF are +3.3 MPa in tension and -3 MPa in compression.

Based on the present study (section 3), we conclude that the displacements and stresses in the SNSF foundation are acceptable, without excessive values and consequences, compared to the full action of the vertical gravity loads of 3116 kN (not presented here).

5. Conclusions

The present paper aims to contribute to a better understanding of the mechanical behavior of a particular shallow foundation called SNSF (Spider Net System Footing). We consider a real particular building situation and propose to study a representative cell involving two layers of soil, the SNSF made of ribs and plates and two columns supporting four floors.

We first study the free vibrations of the cell to evaluate the influence of the supporting soil +SNSF foundation on the lowest frequencies, compared to the upper structure alone. Then we simulate the behavior of the cell under equivalent seismic loads following the methods proposed by the EC8 or ACI codes. Again, we focus on the role of the SNSF foundation on the displacements and stresses in the whole construction system.

Our FEM approach is mainly based on 3D elasticity and the use of advanced commercial codes (Hyperworks of Altair, and Revit of Autodesk). Those tools need skilled engineers and good computer ressources. Hence a second aspect of the paper was to propose a very simple Matlab model based on 2D "brochette" elements in order to evaluate the order of magnitude of some global quantities such as total displacements (energies) on columns, or lowest free frequencies, taking into account the soil-structure interaction. Those simple Matlab models appear helpful and relevant, but the quantification of stresses in the SNSF structure needs 3D FEM models.

Acknowledgments

The scholarship to the first author, provided by the Islamic Bank of Development during the project "UNTIRTA food security" is duly acknowledged.

References

ACI 318M-14 (2015), Building Code Requirements for Reinforced Concrete, American Concrete Institute, Farmington Hills, MI, USA.

Altair Hyperworks Platform (2017), https://www.altair.com/hyperworks/

Bathe, K.J. (2014), *Finite Element Procedures*, 2nd Edition, K.J. Bathe, Watertown, MA.

Batoz, J.L. and Dhatt, G. (1990), *Modélisation des Structures par Eléments Finis*, Volume 2, Poutres et Plaques, Hermès, Paris.

Batoz, J.L., Antaluca, E. and Lamarque, F. (2022), "The finite element modelling of a rectangular slab lying on multilayer elastic soil", *Conference on Broad Exposure to Science and Technology 2021 (BEST 2021)*, Atlantis Press.

Charney, F.A. (2015), *Seismic Loads: Guide to the Seismic Load Provisions of ASCE 7-10*, ASCE Press, Reston, Virginia.

Corvez, D. and Davidovici, V. (2016), Pratique du Calcul Sismique: Guide d'application de l'Eurocode 8, Editions Eyrolles.

Cuira, F. and Simon, B. (2008), "Modélisation 3D simplifiée d'une plaque sur sol multicouche élastique", *Revue Française de Géotechnique*, **124**, 3-17. https://doi.org/10.1051/geotech/2008124003.

Darjanto, H. (2015), "Load transfer mechanisms in the cell spider net system footing construction through full-scale static and cyclical vertical loads and 3d numerical analysis", PhD Dissertation, Diponegoro University.

Darjanto, H., Irsyam, M. and Retno, S.P. (2015), "Full scale static load test on the spider net system", *Jurnal Teknologi*, **77**(11), 73-82. https://doi.org/10.11113/jt.v77.6424.

El Sawwaf, M., Nazir, A., Azzam, W. and Mohy, A. (2017), "Utilization of embedded ribs for improving the bearing capacity of raft foundation in sand", *International Conference on Advances in Structural and Geotechnical Engineering*, Hurghada, Egypt, April.

Eurocode 8 (2004), Design of Structures for Earthquake Resistance, European Committee for Standardization, Brussels, Belgium.

Ibrahimbegović, A. (2009), *Nonlinear Solid Mechanics: Theoretical Formulations and Finite Element Solution Methods*, Springer Dordrecht, Netherlands.

Jalil, W. and Jalil, A. (2014), Conception et analyse sismiques du bâtiment: guide d'application de l'Eurocode 8 à partir des règles PS 92-2004, Paris La Plaine-Saint-Denis: Eyrolles Afnor éd (Eurocode).

Katama, www.katama.co.id (Accessed: 15 February 2022).

Ponginan, R. (2018), *Learn Dynamic Analysis with Altair OptiStruct*, Altair University.

Revit, Robot Structural Analysis (2020), https://www.autodesk.com.

SNI 1726 (2019), Earthquake Resistance Design for Buildings, Indonesian Standard Code.

Soelarso, S., Antaluca, E., Batoz, J.L. and Lamarque, F. (2019), "On the finite element bearing capacity analysis of a rib system to be used as shallow foundation construction", *IOP Conf. Ser.: Mater. Sci. Eng.*, **673**(1), 012030. https://doi.org/10.1088/1757-899X/673/1/012030.

Soelarso, S., Antaluca, E., Batoz, J.L. and Lamarque, F. (2021), "On the finite element modeling of a particular shallow foundation system for soft soil", *Couple. Syst. Mech.*, **10**(3), 247-261. https://doi.org/10.12989/csm.2021.10.3.247.